AIChE

Integrated Batch-to-Batch and Nonlinear Model Predictive Control for Polymorphic Transformation in Pharmaceutical Crystallization

Martin Wijaya Hermanto
Dept. of Chemical and Biomolecular Engineering, National University of Singapore, Singapore 117576

Richard D. Braatz
Dept. of Chemical and Biomolecular Engineering, University of Illinois at Urbana-Champaign, IL 61801

Min-Sen Chiu
Dept. of Chemical and Biomolecular Engineering, National University of Singapore, Singapore 117576

DOI 10.1002/aic.12331
Published online July 20, 2010 in Wiley Online Library (wileyonlinelibrary.com).

Polymorphism, a phenomenon in which a substance can have more than one crystal form, is a frequently encountered phenomenon in pharmaceutical compounds. Different polymorphs can have very different physical properties such as crystal shape, solubility, hardness, color, melting point, and chemical reactivity, so that it is important to ensure consistent production of the desired polymorph. In this study, an integrated batch-to-batch and nonlinear model predictive control (B2B-NMPC) strategy based on a hybrid model is developed for the polymorphic transformation of L-glutamic acid from the metastable α-form to the stable β-form crystals. The hybrid model comprising of a nominal first-principles model and a correction factor based on an updated PLS model is used to predict the process variables and final product quality. At each sampling instance during a batch, extended predictive self-adaptive control (EPSAC) is employed as a NMPC technique to calculate the control action by using the current hybrid model as a predictor. At the end of the batch, the PLS model is updated by utilizing the measurements from the batch and the above procedure is repeated to obtain new control actions for the next batch. In a simulation study using a previously reported model for a polymorphic crystallization with experimentally determined parameters, the proposed B2B-NMPC control strategy produces better performance, where it satisfies all the state constraints and produces faster and smoother convergence, than the standard batch-to-batch strategy.
 AIChE J, 57: 1008–1019, 2011
Keywords: pharmaceutical crystallization, batch-to-batch control, hybrid model, nonlinear model predictive control, extended predictive self-adaptive control

Introduction

Most drug manufacturing processes include a series of crystallizations in which the product crystals are characterized in terms of the crystal size and shape distribution. The

Additional Supporting Information may be found in the online version of this article.

Correspondence concerning this article should be addressed to M.-S. Chiu at checms@nus.edu.sg.

control of polymorphism, also important is which occurs when a molecule can have more than one crystal form.[1–3] Each crystal form has different physical properties such as crystal shape, solubility, hardness, melting point, and chemical reactivity, which makes polymorphism an important consideration when manufacturing crystals for the food, speciality chemical, and pharmaceutical industries where products are specified not only by chemical composition, but also by performance.[1] As a result, ensuring consistent production of the desired polymorph is very important in those industries, especially in drug manufacturing where safety is of critical importance.

The vast majority of articles on crystallization control have considered nonpolymorphic systems in which the control of some characteristic (e.g., weight mean size) of the crystal size distribution was considered. Most studies have investigated the computation of an optimal temperature profile during cooling crystallization by minimizing/maximizing an objective function based on an off-line process model. Although simple to implement, it is well-known that such optimal control policies can be very sensitive to variations in kinetic parameters.[4] While fixed-trajectory optimal temperature control algorithms have been developed to provide robustness to parameter variations, such algorithms will always have some degradation in nominal performance.[5,6] In recent years, concentration control algorithms have been developed that are less sensitive to disturbances and variations in kinetic parameters.[3,7,8] However, both the temperature and concentration control algorithms for crystallization processes are inherently sensitive to shifts in the solubility curve.[8] Such shifts occur in practice, because of variations in the contaminant profiles in the chemical feedstocks.

Due to plant-model mismatch, optimal control obtained from an off-line process model is often suboptimal when applied to the real process. Exploiting the repetitive nature of most batch processes, batch-to-batch control uses results from previous batches to iteratively compute the optimal operating conditions for each batch. Batch-to-batch control has been studied extensively in the past decade. Zafiriou et al.[9] proposed an approach for modifying the input sequence from batch to batch to deal with plant-model mismatch. Their approach is based on an analogy between the iteration during numerical optimization of an objective function and successive batches during the operation of the plant. Clarke-Pringle and MacGregor[10] proposed a method to correct the manipulated variable trajectories from batch to batch with application to the optimization of molecular weight distribution in a polymerization process. The method uses errors between the measured and desired molecular weight distributions at the end of a batch to update the manipulated variable trajectories for the next batch. Lee and co-workers[11] presented the quadratic criterion-based iterative learning control (Q-ILC) approach for tracking control of batch processes based on a linear time-varying (LTV) tracking error transition model. Doyle and coworkers[12,13] used batch-to-batch optimization to achieve the desired particle size distribution (PSD) target in an emulsion polymerization reactor. A simplified theoretical model is used as predictor, but the prediction is corrected using an updated PLS model that relates the manipulated variables to the error from the theoretical model prediction and the measured distribution. Xiong and Zhang[14] presented a recurrent neural network-based ILC scheme for batch processes where the filtered recurrent neural network prediction errors from previous batches are added to the model predictions for the current batch and the updated predictions used in optimization. Li et al.[15] presented batch-to-batch optimal control in which a batchwise recursive nonlinear PLS algorithm updates the model after each batch.

With the ability of model predictive control (MPC) to respond to disturbances occurring during the batch and batch-to-batch control to correct bias left uncorrected by the MPC, combining both methods to obtain better control performance is possible. This integrated control strategy can combine information from the past error tracking signals with that from the current batch to adjust the manipulated variable trajectories more effectively in real time. If disturbances occur, the integrated control method is expected to more rapidly counteract the effect of disturbances than batch-to-batch control only. Lee and coworkers[16–18] proposed a batch MPC (BMPC) technique for tracking control by incorporating the capability of real-time feedback control into Q-ILC. Chin et al.[19] proposed a two-stage control framework by combining the Q-ILC and BMPC methods to separately handle the real-time disturbance and the batchwise persisting disturbance, respectively.

The aforementioned integrated control strategies[16–19] rely on LTV models, which can have poor extrapolative capability. Motivated by this and the benefits of the integrated control strategy, an integrated batch-to-batch and nonlinear MPC (B2B-NMPC) control algorithm is proposed that employs a hybrid model consisting of the nominal first-principles model and a correction factor obtained from an updated PLS model. A major benefit of the hybrid model is the ability to harness the extrapolative capability of the first-principles model, whereas the PLS model provides a means for simple model updating. The NMPC algorithm is based on extended predictive self-adaptive control (EPSAC)[20–23] to perform on-line control to handle the constraints effectively, whereas the batch-to-batch control refines the model by learning from the previous batches. In a simulation study, the proposed control strategy results in improved constraint handling and faster and smoother convergence compared with the standard batch-to-batch control strategy. The next section summarizes the process description for polymorphic crystallization of L-glutamic acid. This is followed by the development of the batch-to-batch control strategy based on the aforementioned hybrid model. The integration of NMPC into the batch-to-batch control is presented next. Finally, simulation results are presented for the implementation of the control strategies to the polymorphic transformation of L-glutamic acid from the metastable α-form to the stable β-form crystals. Then conclusions are presented.

Description of Polymorphic Crystallization Process

This section summarizes the polymorphic crystallization model for metastable α-form and stable β-form crystals of L-glutamic acid, which was recently developed by the authors.[24] The conservation equations for the crystals are population balance equations:

$$\frac{\partial f_{\text{seed},i}}{\partial t} + \frac{\partial\left(G_i f_{\text{seed},i}\right)}{\partial L} = 0, \tag{1}$$

$$\frac{\partial f_{\text{nucl},i}}{\partial t} + \frac{\partial\left(G_i f_{\text{nucl},i}\right)}{\partial L} = B_i \delta(L - L_0), \tag{2}$$

where $f_{\text{seed},i}$ and $f_{\text{nucl},i}$ are the crystal size distributions of the i-form crystals (i.e., α- or β-form crystals) obtained from seed crystals and nucleated crystals [#/m^4], respectively, B_i and G_i are the nucleation [#/m^{3}s] and growth rate [m/s] of the i-form crystals, respectively, L and L_0 are the characteristic size of crystals [m] and nuclei [m], respectively, and $\delta(\cdot)$ is the Dirac delta function. The mass balance on the solute is

$$\frac{dC}{dt} = -\frac{3 \times 10^3}{\rho_{\text{solv}}}\left(\rho_\alpha k_{v\alpha} G_\alpha \mu_{\alpha,2} + \rho_\beta k_{v\beta} G_\beta \mu_{\beta,2}\right), \tag{3}$$

where the nth moment of the i-form crystals [# m^{n-3}] is given by

$$\mu_{i,n} = \int_0^\infty L^n (f_{\text{nucl},i} + f_{\text{seed},i}) dL, \tag{4}$$

C is the solute concentration [g/kg], ρ_{solv} is the density of the solvent [kg/m^3], ρ_i is the density of the i-form crystals [kg/m^3], k_{vi} is the volumetric shape factor of the i-form crystals (dimensionless) as defined by $v_i = k_{vi} L^3$ where v_i is the volume of the i-form crystal [m^3], and 10^3 is a constant [g/kg] to ensure unit consistency. The kinetic expressions are

$$B_\alpha = k_{b\alpha}(S_\alpha - 1)\mu_{\alpha,3} \qquad (\alpha\text{-form crystal nucleation rate}), \tag{5}$$

$$G_\alpha = \begin{cases} k_{g\alpha}(S_\alpha - 1)^{g_\alpha} & \text{if } S_\alpha \geq 1 \\ k_{d\alpha}(S_\alpha - 1) & \text{otherwise} \end{cases} \quad (\alpha\text{-form crystal growth/dissolution rate}), \tag{6}$$

$$B_\beta = k_{b\beta,1}(S_\beta - 1)\mu_{\alpha,3} + k_{b\beta,2}(S_\beta - 1)\mu_{\beta,3} \quad (\beta\text{-form crystal nucleation rate}), \tag{7}$$

$$G_\beta = k_{g\beta,1}(S_\beta - 1)^{g_\beta} \exp\left(-\frac{k_{g\beta,2}}{S_\beta - 1}\right) \quad (\beta\text{-form crystal growth rate}), \tag{8}$$

where $S_i = C/C_{\text{sat},i}$ and $C_{\text{sat},i} = a_{i,1}T^2 + a_{i,2}T + a_{i,3}$ are the supersaturation and the saturation concentration [g/kg] of the i-form crystals, respectively, and T is the solution temperature [°C]. The kinetic parameters $k_{b\alpha}$, $k_{g\alpha}$, and $k_{d\alpha}$ correspond to the nucleation [#/m^{3}s], growth [m/s], and dissolution [m/s] rates of α-form crystals, respectively, whereas $k_{b\beta,j}$ and $k_{g\beta,j}$ correspond to the jth nucleation [#/m^{3}s] and growth [m/s] for $j = 1$ and dimensionless for $j = 2$ rates of β-form crystals, respectively, and g_i is the growth exponential constant of the i-form crystals, which may have a value between 1 (for diffusion-limited growth) and 2 (for surface integration-limited growth).[25] The Arrhenius equation was used to account for the variability of the crystal growth rate with temperature:

$$k_{g\alpha} = k_{g\alpha,0} \exp\left(-\frac{E_{g\alpha}}{8.314(T + 273)}\right), \tag{9}$$

Table 1. Model parameters for the Polymorphic Crystallization of L-glutamic acid

Parameters	Values	Parameters	Values
$\ln k_{b\alpha}$	17.233	ρ_{solv}	990
$\ln k_{g\alpha,0}$	1.878	ρ_α	1540
g_α	1.859	ρ_β	1540
$\ln E_{g\alpha}$	10.671	$k_{v\alpha}$	0.480
$\ln k_{d\alpha}$	−10.260	$k_{v\beta}$	0.031
$\ln k_{b\beta,1}$	15.801	$a_{\alpha,1}$	8.437×10^{-3}
$\ln k_{b\beta,2}$	20.000	$a_{\alpha,2}$	0.03032
$\ln k_{g\beta,0}$	52.002	$a_{\alpha,3}$	4.564
$\ln k_{g\beta,2}$	−0.251	$a_{\beta,1}$	7.644×10^{-3}
g_β	1.047	$a_{\beta,2}$	−0.1165
$\ln E_{g\beta}$	12.078	$a_{\beta,3}$	6.622

$$k_{g\beta,1} = k_{g\beta,0} \exp\left(-\frac{E_{g\beta}}{8.314(T + 273)}\right), \tag{10}$$

where $k_{gi,0}$ and E_{gi} are the pre-exponential factor [m/s] and activation energy [J/mol] for the growth rate of i-form crystals, respectively. The nominal values for the model parameters are given in Table 1. To solve the system equations (1–10), the JSHWENO discretization method detailed in Hermanto et al.[26] was employed.

Two on-line measurements considered in this study are the crystallizer temperature and solute concentration. The temperature measurements are readily available using thermocouples. Several on-line techniques are available for measuring solution concentration such as conductivity or attenuated total reflection Fourier transform infrared spectroscopy.[27,28] The final product quality for the polymorphic transformation of α- to β-form crystals is characterized in two different ways. One objective is to maximize the third-order moment of β-form crystals:

$$P_1 = \mu_{\beta,3}(t_f), \tag{11}$$

which is the same as maximizing the yield of β-form crystals and t_f is the batch time. The second objective is to minimize the nucleated crystal mass to seed crystal mass ratio of β-form crystals:

$$P_2 = \frac{\mu_{\beta,3}^{\text{nucl}}(t_f)}{\mu_{\beta,3}^{\text{seed}}(t_f)}. \tag{12}$$

The optimization is subject to the model equations and the inequality constraints:

$$T_{\min} \leq T(t) \leq T_{\max}, \tag{13}$$

$$C_{\text{sat},\beta}(t) \leq C(t) < C_{\text{sat},\alpha}(t), \tag{14}$$

$$C(t_f) \leq C_{\max}(t_f), \tag{15}$$

where $T_{\min} = 25°$ C and $T_{\max} = 50°$ C are the minimum and maximum allowed temperatures. The inequality constraint (14) aims to avoid the nucleation and growth rate of α-form crystals and the dissolution of β-form crystals during the polymorphic transformation. The end-point inequality constraint (15) ensures that the minimum yield required by economic considerations is satisfied.

Batch-to-Batch (B2B) Control Strategy

The batch-to-batch control strategy is based on a hybrid model consisting of a first-principles model and a PLS model. This approach exploits the improved extrapolative ability of a first-principles model while the inevitable modeling error is corrected through a PLS model using data from previous batches. For any process variables of interest (such as the product quality and constrained variables) at the kth sampling instance of the jth batch, z_k^j, its prediction can be decomposed into two factors:

$$z_k^j = z_{\mathrm{fp},k}^j + \Delta z_{\mathrm{pls},k}^j, \tag{16}$$

where $z_{\mathrm{fp},k}^j$ is obtained from the first-principles model with nominal model parameters and $\Delta z_{\mathrm{pls},k}^j$ is the correction obtained from the PLS model using the quadratic PLS (QPLS)[29] technique.

Generally, the PLS method reduces the dimension of the predictor variables $\mathbf{X} \in \mathbb{R}^{n \times n_x}$ and response variables $\mathbf{Y} \in \mathbb{R}^{n \times n_y}$, where n, n_x, n_y denote the respective numbers of datasets, input, and output variables, by projection to directions that maximize the covariance between input and output variables. The decompositions of $\mathbf{X}$ and $\mathbf{Y}$ into their score and loading matrices are

$$\mathbf{X} = \mathbf{S}\mathbf{O}^T + \mathbf{E} = \sum_{h=1}^{n_{\mathrm{latent}}} \mathbf{s}_h \mathbf{o}_h^T + \mathbf{E}, \tag{17}$$

$$\mathbf{Y} = \mathbf{U}\mathbf{Q}^T + \mathbf{F} = \sum_{h=1}^{n_{\mathrm{latent}}} \mathbf{u}_h \mathbf{q}_h^T + \mathbf{F}, \tag{18}$$

where $\mathbf{S} \in \mathbb{R}^{n \times n_{\mathrm{latent}}}$ and $\mathbf{U} \in \mathbb{R}^{n \times n_{\mathrm{latent}}}$ are the score matrices for $\mathbf{X}$ and $\mathbf{Y}$, respectively, $\mathbf{O} \in \mathbb{R}^{n_x \times n_{\mathrm{latent}}}$ and $\mathbf{Q} \in \mathbb{R}^{n_y \times n_{\mathrm{latent}}}$ are the loading matrices for $\mathbf{X}$ and $\mathbf{Y}$, respectively, $\mathbf{E}$ and $\mathbf{F}$ are matrices of residuals, $\mathbf{s}_h$, $\mathbf{o}_h$, $\mathbf{u}_h$, and $\mathbf{q}_h$ are the hth columns of matrices $\mathbf{S}$, $\mathbf{O}$, $\mathbf{U}$, and $\mathbf{Q}$, respectively, and n_{latent} is the number of the specified latent variables. In the conventional PLS approach, the score vectors $\mathbf{s}_h$ and $\mathbf{u}_h$ are related linearly. In contrast, in QPLS the vectors are related quadratically by

$$\mathbf{u}_h = c_{0h} + c_{1h}\mathbf{s}_h + c_{2h}\mathbf{s}_h^2 + \varepsilon_h, \tag{19}$$

where c_{jh} is the jth regression coefficient, ε_h is the residual vector, and $\mathbf{s}_h^2$ is the vector in which each element is the square of the corresponding element of $\mathbf{s}_h$.

The first step to obtain $\Delta z_{\mathrm{pls},k}^j$ is to prepare the matrices $\mathbf{X}$ and $\mathbf{Y}$ from the historical database. Each row of the matrix $\mathbf{X}$ consists of the input variables (i.e., temperature in this article) at sampling instances 0 to $k-1$ for a particular batch, while each row of the matrix $\mathbf{Y}$ contains the deviation between a real process variable (i.e., solute concentration at each sampling instance k and product quality at the end of each batch) and that predicted by the first-principles model in the same batch. Note that the solute concentration prediction is used to handle solute concentration constraints (14) and (15). There are two common approaches to determine the number of datasets (n) kept in the database. The first approach is to keep the datasets from all past batches (n increases every batch) and the other approach is to keep only the datasets from the latest n batches (i.e., the moving window approach).

The second step to obtain $\Delta z_{\mathrm{pls},k}^j$ is to decompose both database matrices into their corresponding score and loading vectors. The regression coefficients are obtained by the QPLS algorithm as detailed elsewhere.[29] In this study, n_{latent} is chosen as the maximum number such that the explained variances in matrices $\mathbf{X}$ and $\mathbf{Y}$ do not exceed 99%.

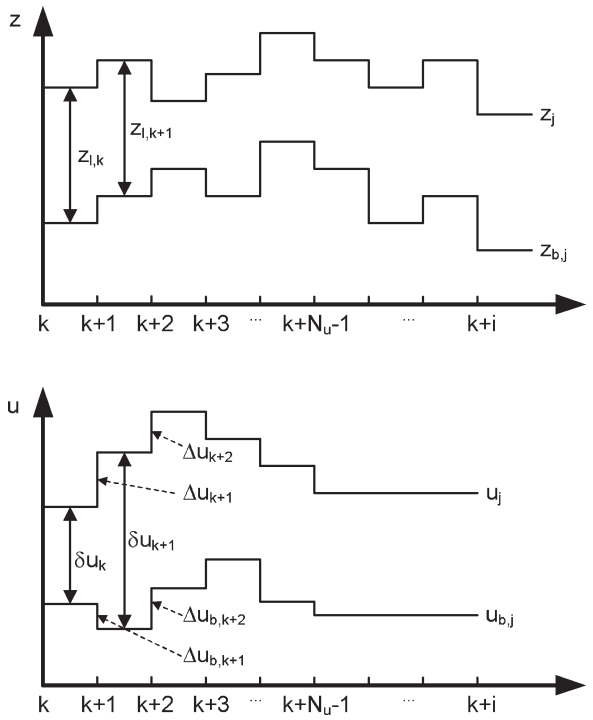

Figure 1. The decomposition of variables in EPSAC.

For a new input vector $\mathbf{x}_{\mathrm{pls}}$, the output correction term $\Delta z_{\mathrm{pls},k}^j$ is obtained as follows:

(1) Arrange the elements in the row vector $\mathbf{x}_{\mathrm{pls}}$ in the same manner as for the database matrix $\mathbf{X}$.

(2) For $h = 1,\ldots,n_{\mathrm{latent}}$, calculate the contributions to the output vector $\mathbf{y}_{\mathrm{pls}h}$ as follows:

(a) Obtain the input score vector $\hat{\mathbf{s}}_h$ corresponding to the new input vector from

$$\hat{\mathbf{s}}_h = \frac{\mathbf{x}_{\mathrm{pls}}\mathbf{o}_h}{\mathbf{o}_h^T\mathbf{o}_h}.$$

(b) Calculate the output score vector $\hat{\mathbf{u}}_h$ from

$$\hat{\mathbf{u}}_h = c_{0h} + c_{1h}\hat{\mathbf{s}}_h + c_{2h}\hat{\mathbf{s}}_h^2,$$

where each element of $\hat{\mathbf{s}}_h^2$ is the square of the corresponding element of $\hat{\mathbf{s}}_h$.

(c) Obtain the residuals vector $\mathbf{e}$ from

$$\mathbf{e} = \mathbf{x}_{\mathrm{pls}} - \hat{\mathbf{s}}_h\mathbf{o}_h^T,$$

and set $\mathbf{x}_{\mathrm{pls}} = e$ for the next dimension $h = h + 1$.

(3) Calculate the output correction term from

$$\Delta z_{\mathrm{pls},k}^j = \sum_{h=1}^{n_{\mathrm{latent}}} \hat{\mathbf{u}}_h \mathbf{q}_h^T.$$

In the batch-to-batch control strategy, the objective function to be minimized before the jth batch is

Table 2. The Parameters Describing the Size Distributions of Seed Crystals

Seed form	Mass [g]	Mean crystal size [μ m]	Standard deviation of crystal size [μ m]
α	10.0	100.0	10.0
β	1.0	100.0	10.0

$$J_{\mathrm{B2B}} = \min_{\mathcal{U}} \left[W_p (P - P_d)^2 + \Delta\mathcal{U}^T \mathbf{W}_{\Delta\mathcal{U}} \, \Delta\mathcal{U} + \mathrm{d}\mathcal{U}^{\mathrm{T}} \mathbf{W}_{\mathrm{d}\mathcal{U}} \mathrm{d}\mathcal{U} \right], \tag{20}$$

subject to process model and inequality constraints (13–15), and

$$\mathcal{U} = \left[u_0^j, u_1^j, \ldots, u_{N-1}^j \right]^T,$$
$$\Delta\mathcal{U} = \left[u_1^j - u_0^j, u_2^j - u_1^j, \ldots, u_{N-1}^j - u_{N-2}^j \right]^T,$$
$$\mathrm{d}\mathcal{U} = \left[u_0^j - u_0^{j-1}, u_1^j - u_1^{j-1}, \ldots, u_{N-1}^j - u_{N-1}^{j-1} \right]^T,$$

and P and P_d are the predicted and desired final product quality, given by either (11) or (12), u_k^j is the input value at the kth sampling instance of the jth batch, N is the total number of samples in one batch, W_p is a scalar weight on the final product quality, and $\mathbf{W}_{\Delta\mathcal{U}}$ and $\mathbf{W}_{\mathrm{d}\mathcal{U}}$ are weight matrices used to penalize excessive changes in the input variable, which occur within a batch and between batches, respectively. In (20), P_d is equal to 0 if the objective is to minimize P. To maximize P, the minus of the summation term inside the square bracket is minimized in addition to setting $P_d = 0$. The differential evolution (DE)[30,31] method was used to numerically solve the minimization problem before every batch, where P was computed using the simulation method described in the previous section. DE belongs to the class of evolution strategy optimizers (e.g., genetic algorithms, particle swarm optimization). DE generates a new individual from the population by taking vector differences between other randomly selected members of the population, which avoids the use of any separate probability distributions. DE was used because, it is easy to implement and is one of the faster stochastic optimization algorithms.

Integrated Batch-to-Batch and NMPC (B2B-NMPC) Control Strategy

The main shortcoming of batch-to-batch control strategy lies in its open-loop nature, where the correction is not made until the next batch. As a result, its capability to handle constraints for the current batch solely depends on the accuracy of the corrected model from the previous batch. When the corrected model is not accurate, which is likely the case in the first few batches, the constraints can become violated when the input values are implemented. If on-line measurement of some process variables are available, it is possible and beneficial to integrate nonlinear model predictive control (NMPC) into the batch-to-batch control strategy. Both control strategies complement each other such that the NMPC can perform on-line control to handle the constraints effectively, whereas the batch-to-batch control strategy refines the model by learning from the previous batches.

In this integrated B2B-NMPC control strategy, the formulation of the hybrid model remains the same, except that the definition of the matrix $\mathbf{X}$ in the PLS model includes both the input and measured process variables (that is, the temperature and solute concentration measurements) available at sampling instances 0 to $k - 1$. Contrary to B2B control strategy, solute concentration measurements are included in matrix $\mathbf{X}$ to improve the model prediction accuracy, as the new input vector $\mathbf{x}_{\mathrm{pls}}$ can utilize the online solute concentration measurements in this case. Note that the matrix $\mathbf{X}$ only includes data from the previous batches (that is, excluding data from the current batch) because inclusion of data from the current batch in the database would need the corresponding output $\mathbf{Y}$ of the current batch, which is not available.

The NMPC strategy is based on EPSAC,[20–23] in which the main idea is to approximate nonlinear process variables by iterative linearization around future trajectories so as to converge to the same optimal solution. In the subsequent discussion of EPSAC, the superscript j indicating the current batch index is mostly dropped to simplify notation. In EPSAC, the future sequence of the input variable u_{k+i} is defined by (see Figure 1):

$$u_{k+i} = u_{b,k+i} + \delta u_{k+i}, \quad i = 0, 1, \ldots, N_u - 1, \tag{21}$$

where $u_{b,k+i}$ is the predetermined future control scenario, δu_{k+i} is the optimizing future control actions, N_u is the control horizon, and

$$\Delta u_{l,k} = \delta u_k,$$
$$\delta u_{k+m} = \sum_{j=0}^{m} \Delta u_{l,k+j}.$$

The future trajectory of any process variables of interest (z_{k+i}) can be treated as being the cumulative result of two effects:

Table 3. Perturbations in the Process Parameters for the Robustness study

Cases	$\ln k_{b\beta,1}$	$\ln k_{b\beta,2}$	$\ln k_{g\beta,0}$	$\ln k_{g\beta,2}$	g_β	$\ln E_{g\beta}$
1	15.758	19.961	53.200	−0.280	1.100	12.060
2	15.842	20.036	50.883	−0.240	1.019	12.070

Case 1 has slow nucleation and fast growth rate parameters for the β-form crystals and Case 2 has fast nucleation and slow growth rate parameters for the β-form crystals.

Table 4. Tuning Parameters for the B2B Control Strategy*

Values for objective J_1	Values for objective J_2
$W_{p,1} = 1$	$W_{p,2} = 1$
$(\mathbf{W}_{\Delta\mathcal{U},1})_{i,i} = 2[1 + 15(\mathrm{i} - 1)] \times 10^{-5}$	$(\mathbf{W}_{\Delta\mathcal{U},2})_{i,i} = 3[1 + 0.5(i - 1)] \times 10^{-5}$
$\mathbf{W}_{\mathrm{d}\mathcal{U},1} = 3 \times 10^{-5} I$	$\mathbf{W}_{\mathrm{d}\mathcal{U},2} = 5 \times 10^{-6} I$
$\mathbf{W}_\epsilon = 10I$	$\mathbf{W}_\epsilon = 10I$
$\mathbf{W}_\epsilon = 10[1,1,\ldots,1]^T$	$\mathbf{W}_\epsilon = 10[1,1,\ldots,1]^T$

*$\mathbf{W}_{\Delta\mathcal{U},1}$ and $\mathbf{W}_{\Delta\mathcal{U},2}$ are diagonal $N \times N$ matrices.

Table 5. Tuning Parameters for the B2B-NMPC Control Strategy*

Values for objective J_1	Values for objective J_2
$W_{p,1} = 1$	$W_{p,2} = 1$
$(\mathbf{W}_{\Delta\mathrm{U},1})_{i,i} = [1 + 15(i - 1)] \times 10^{-5}$	$(\mathbf{W}_{\Delta\mathrm{U},2})_{i,i} = 9[1 + 0.7(i - 1)] \times 10^{-5}$
$\mathbf{W}_{\mathrm{dU},1} = 1.5 \times 10^{-5} I$	$\mathbf{W}_{\mathrm{dU},2} = 6 \times 10^{-6} I$
$\mathbf{W}_\epsilon = 10I$	$\mathbf{W}_\epsilon = 10I$
$\mathbf{w}_\epsilon = 10[1,1,\ldots,1]^T$	$\mathbf{w}_\epsilon = 10[1,1,\ldots,1]^T$

*$\mathbf{W}_{\Delta\mathrm{U},1}$ and $\mathbf{W}_{\Delta\mathrm{U},2}$ are diagonal $(N - k) \times (N - k)$ matrices.

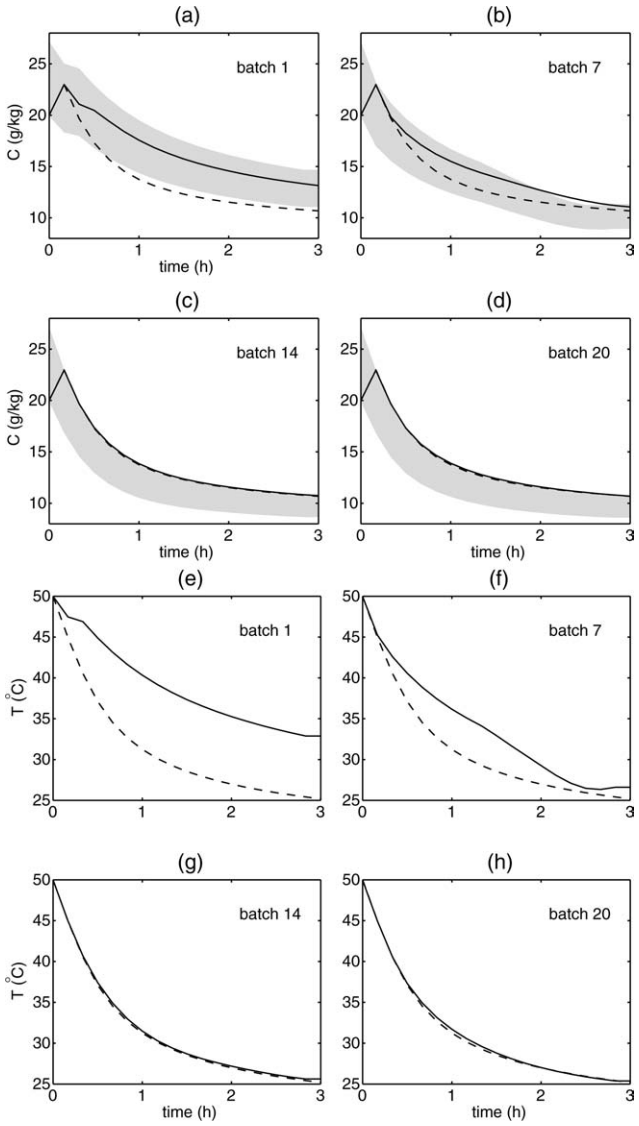

Figure 2. The results of applying the B2B control strategy for Case 1 and objective J_1 for batches 1, 7, 14, and 20.

(a)–(d) concentration trajectories with the shading showing the feasible region for the concentration; (e)–(h) the corresponding temperature trajectories. Solid line: B2B control, dashed line: optimal control.

$$z_{k+i} = z_{b,k+i} + z_{l,k+i}, \tag{22}$$

where $z_{b,k+i}$ is calculated using the hybrid model (16) with predetermined sequence $u_{b,k+i}$, and

$$z_{l,k+i} = g_i \Delta u_{l,k} + g_{i-1} \Delta u_{l,k+1} + \cdots + g_{i-N_u+1} \Delta u_{l,k+N_u-1}. \tag{23}$$

is determined by the optimized future control actions, where g_j is the jth step response coefficients.

Considering a batch process with the control horizon identical to the prediction horizon, which covers from the next sampling instance to the end of batch time denoted by $N_p = N_u = N - k$, the future process variable of interest in the prediction horizon can be conveniently represented as

$$\mathbf{Z} = \mathbf{Z}_b + \mathbf{G}_l \Delta \mathbf{U}_l, \tag{24}$$

where

$$\mathbf{Z} = [z_{k+1}, z_{k+2}, \ldots, z_N]^T,$$
$$\mathbf{Z}_b = [z_{b,k+1}, z_{b,k+2}, \ldots, z_{b,N}]^T,$$
$$\Delta \mathbf{U}_l = [\Delta u_{l,k}, \Delta u_{l,k+1}, \ldots, \Delta u_{l,N-1}]^T,$$
$$\mathbf{G}_l = \begin{bmatrix} g_1 & 0 & \cdots & 0 \\ g_2 & g_1 & \cdots & 0 \\ \vdots & \vdots & \ddots & \vdots \\ g_{N-k} & g_{N-k-1} & \cdots & g_1 \end{bmatrix}.$$

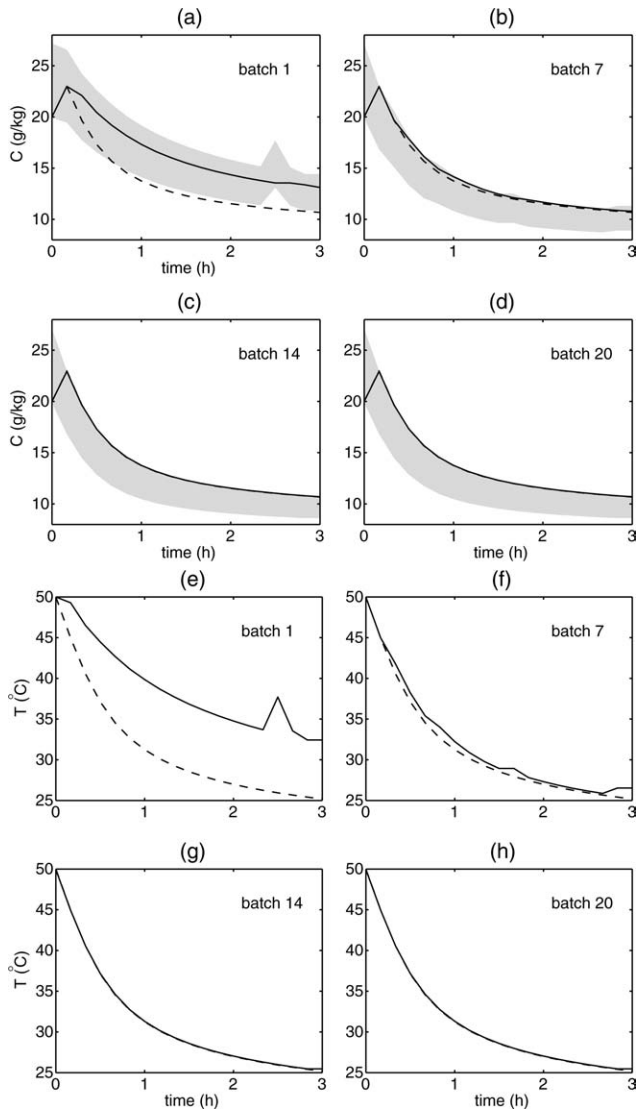

Figure 3. The results of applying the B2B-NMPC control strategy for Case 1 and objective J_1 for batches 1, 7, 14, and 20.

(a)–(d) concentration trajectories with the shading showing the feasible region for the concentration; (e)–(h) the corresponding temperature trajectories. Solid line: B2B-NMPC control, dashed line: optimal control.

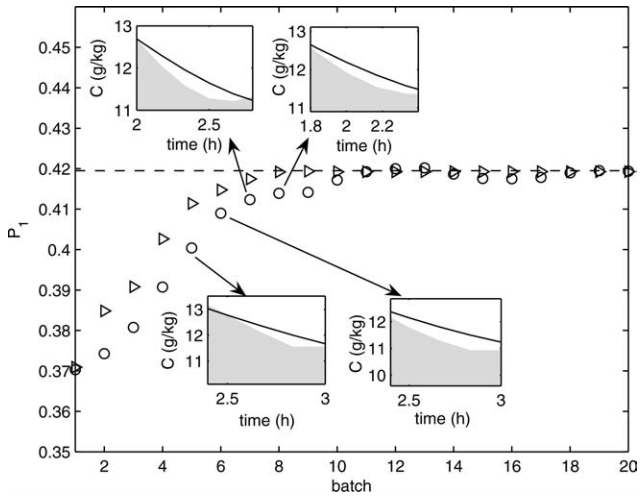

Figure 4. Comparison of the product quality P_1 obtained by the B2B (○) and B2B-NMPC (▷) control strategies for Case 1 and objective J_1.

The insets show the constraint violations for the B2B control strategy in batches 5 to 8.

The objective function optimized at every sampling instance is*

$$J_{\text{B2B-NMPC}} = \min_{\mathbf{U}} \left[W_p (P - P_d)^2 + \Delta\mathbf{U}^T \mathbf{W}_{\Delta\mathbf{U}} \Delta\mathbf{U} + d\mathbf{U}^T \mathbf{W}_{d\mathbf{U}} d\mathbf{U} \right], \tag{25}$$

subject to process model and inequality constraints (13–15), and

$$\mathbf{U} = \left[u_k^j, u_{k+1}^j, \ldots, u_{N-1}^j \right]^T,$$

$$\Delta\mathbf{U} = \left[u_k^j - u_{k-1}^j, u_{k+1}^j - u_k^j, \ldots, u_{N-1}^j - u_{N-2}^j \right]^T,$$

$$d\mathbf{U} = \left[u_k^j - u_k^{j-1}, u_{k+1}^j - u_{k+1}^{j-1}, \ldots, u_{N-1}^j - u_{N-1}^{j-1} \right]^T,$$

and $\mathbf{W}_{\Delta\mathbf{U}}$ and $\mathbf{W}_{d\mathbf{U}}$ are weight matrices used to penalize excessive changes in the the input variable that occur within each batch and between batches, respectively.

Using the representation in (24), P, $\Delta\mathbf{U}$, and $d\mathbf{U}$ in (25) can be written as

$$P = P_b + \mathbf{G}_{pl} \Delta\mathbf{U}_l, \tag{26}$$

$$\Delta\mathbf{U} = \Delta\mathbf{U}_b + \Delta\mathbf{U}_l, \tag{27}$$

$$d\mathbf{U} = \mathbf{U}_b + \mathbf{M}\Delta\mathbf{U}_l - \mathbf{U}_{\text{prev}}, \tag{28}$$

where P_b is the product quality calculated using the hybrid model with predetermined future inputs $\mathbf{U}_b = [u_{b,k}, u_{b,k+1}, \ldots, u_{b,N-1}]^T$, $\mathbf{G}_{pl}$ is the step response coefficient matrix for the product quality, $\Delta\mathbf{U}_b = [\Delta u_{b,k}, \Delta u_{b,k+1}, \ldots, \Delta u_{b,N-1}]^T$ is the change in the predetermined future inputs, $\mathbf{U}_{\text{prev}} = [u_k^{j-1}, u_{k+1}^{j-1}, \ldots, u_{N-1}^{j-1}]^T$ is the input sequence from the previous batch, and M is a lower triangular matrix with all elements equal to one. This allows the minimization problem (25) to be written as

$$J_{\text{B2B-NMPC}} = \min_{\Delta\mathbf{U}_l} \Delta\mathbf{U}_l^T \Gamma \Delta\mathbf{U}_l + \psi^T \Delta\mathbf{U}_l, \tag{29}$$

where

$$\Gamma = W_p \mathbf{G}_{pl}^T \mathbf{G}_{pl} + W_{\Delta\mathbf{U}} + \mathbf{M}^T \mathbf{W}_{d\mathbf{U}} \mathbf{M},$$

$$\psi = 2 \left[W_p (P_b - P_d)^T G_{pl} + \Delta\mathbf{U}_b^T \mathbf{W}_{\Delta\mathbf{U}} + (\mathbf{U}_b - \mathbf{U}_{\text{prev}})^T \mathbf{W}_{d\mathbf{U}} \mathbf{M} \right]^T.$$

Similarly, the inequality constraints (13–15), represented as $\mathbf{H}(\mathbf{U}) \leq 0$, can be written as

$$\mathbf{H}_b + \mathbf{G}_{hl} \Delta\mathbf{U}_l \leq 0, \tag{30}$$

where $\mathbf{G}_{hl}$ is the step response coefficient matrix corresponding to the constraints and $\mathbf{H}_b$ is calculated using the hybrid model (16) with predetermined future inputs $\mathbf{U}_b$. The soft-constraint approach[32] was used, which modifies the optimization to

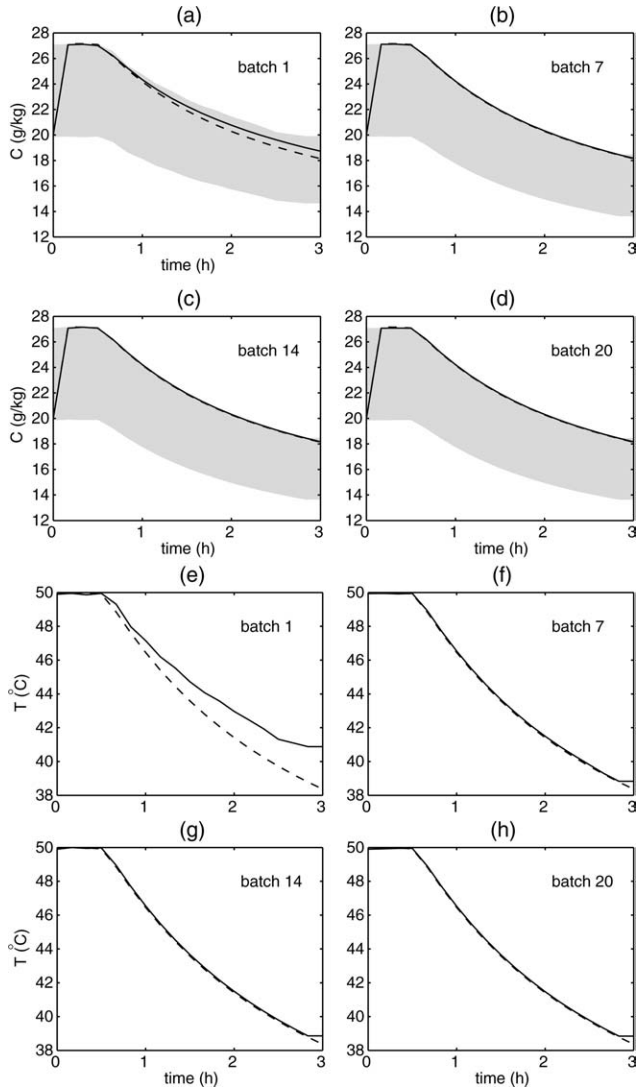

Figure 5. The results of applying the B2B control strategy for Case 2 and objective J_1 for batches 1, 7, 14, and 20.

(a)–(d) concentration trajectories with the shading showing the feasible region for the concentration; (e)–(h) the corresponding temperature trajectories. Solid line: B2B control, dashed line: optimal control.

*The maximization of a product quality objective is converted into the equivalent minimization by multiplying by minus one.

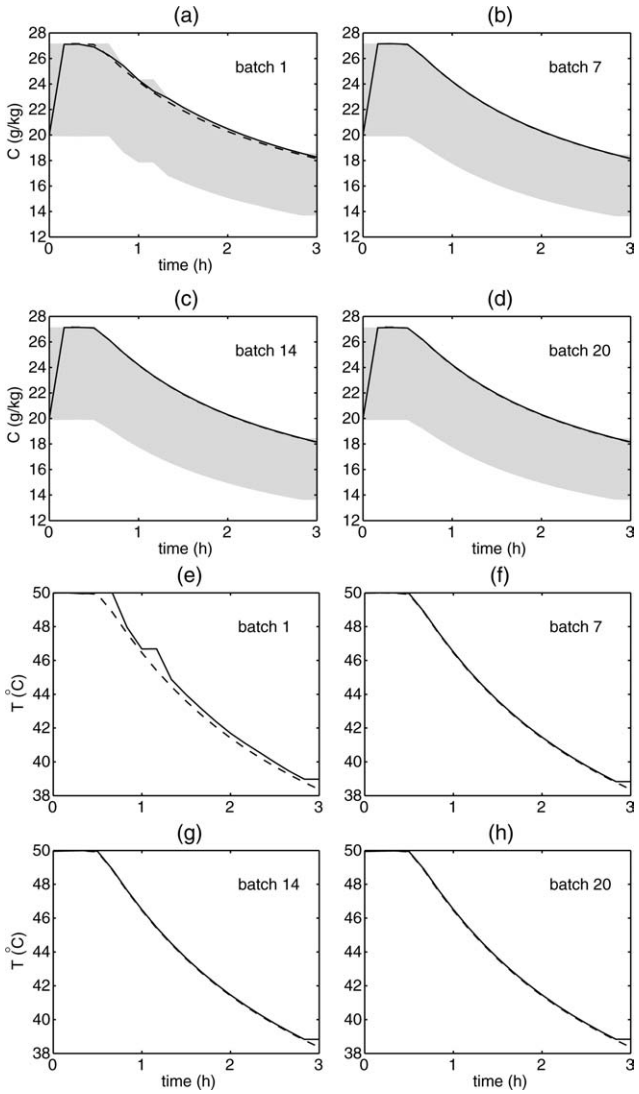

Figure 6. The results of applying the B2B-NMPC control strategy for Case 2 and objective J_1 for batches 1, 7, 14, and 20.

(a)–(d) concentration trajectories with the shading showing the feasible region for the concentration; (e)–(h) the corresponding temperature trajectories. Solid line: B2B-NMPC control, dashed line: optimal control.

$$J^*_{\text{sc,B2B}-\text{NMPC}} = \min_{\Pi} \ \Pi^T \Lambda \Pi + \tau^T \Pi, \tag{31}$$

subject to

$$\begin{bmatrix} \mathbf{H}_b \\ 0 \end{bmatrix} + \begin{bmatrix} \mathbf{G}_{hl} & -\mathbf{I} \\ 0 & -\mathbf{I} \end{bmatrix} \Pi \leq 0, \tag{32}$$

where

$$\Pi = \begin{bmatrix} \Delta \mathbf{U}_l^T & \epsilon^T \end{bmatrix}^T, \qquad \Lambda = \begin{bmatrix} \Gamma & 0 \\ 0 & \mathbf{W}_\epsilon \end{bmatrix},$$
$$\tau = \begin{bmatrix} \psi^T & \mathbf{w}_\epsilon^T \end{bmatrix}^T,$$

ϵ is a vector of slack variables, $\mathbf{W}_\epsilon$ is a diagonal matrix of positive weight, and $\mathbf{w}_\epsilon$ is a vector of positive elements.

In summary, the procedure for implementation of the integrated B2B-NMPC control strategy at the kth sampling instance in the jth batch is

(1) Prepare the database matrices $\mathbf{X}$ and $\mathbf{Y}$ for the PLS model as follows:

- If $j = 1$, the database matrices $\mathbf{X}$ and $\mathbf{Y}$ for the PLS model can be obtained from the historical batch data. Alternatively, input sequences around the nominal trajectory, which is the optimal input sequence for the nominal first-principles model, are implemented to the process and the resulting measurements are used to construct the database.
- If $j > 1$, update the database matrices by including the previous batch measurements dataset into the database. In this study, the moving window approach is adopted, where the dataset from the earliest batch is removed each time a new dataset is included.

(2) Obtain $\mathbf{U}_b$ as follows:

- if $k = 0$ and $iter = 1$, $\mathbf{U}_b$ is chosen to be the input trajectory implemented in the previous batch,
- if $k > 0$ and $iter = 1$, $\mathbf{U}_b$ is set as the $\mathbf{U}_{\text{optimal}}$ obtained in the previous sampling instance of the current batch,
- if $iter > 1$, the updated $\mathbf{U}_b$ from the previous iteration is used,

where $iter$ is the iteration count for updating $\mathbf{U}_b$ at the kth sample instance of the jth batch.

(3) Obtain P_b and $\mathbf{H}_b$ by using $\mathbf{U}_b$ as the input to the hybrid process model. In this study, it was assumed that the constrained variables are measured so that the bias between the predictions and the measurements of the constrained variables at the current sampling instance k were added into the future predictions. If the constrained variables are not measured, then employ state estimation such as extended Kalman filter (EKF) or unscented Kalman filter (UKF) to estimate the constrained variables.

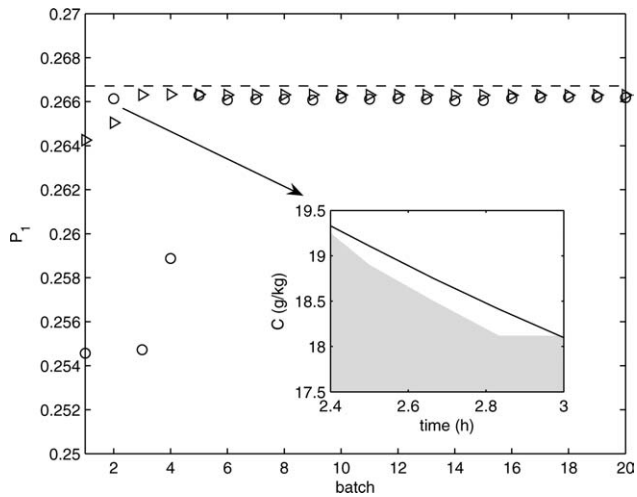

Figure 7. Comparison of the product quality P_1 obtained by the B2B (○) and B2B-NMPC (▷) control strategies for Case 2 and objective J_1.

The inset shows the constraint violations for the B2B control strategy in batch 2.

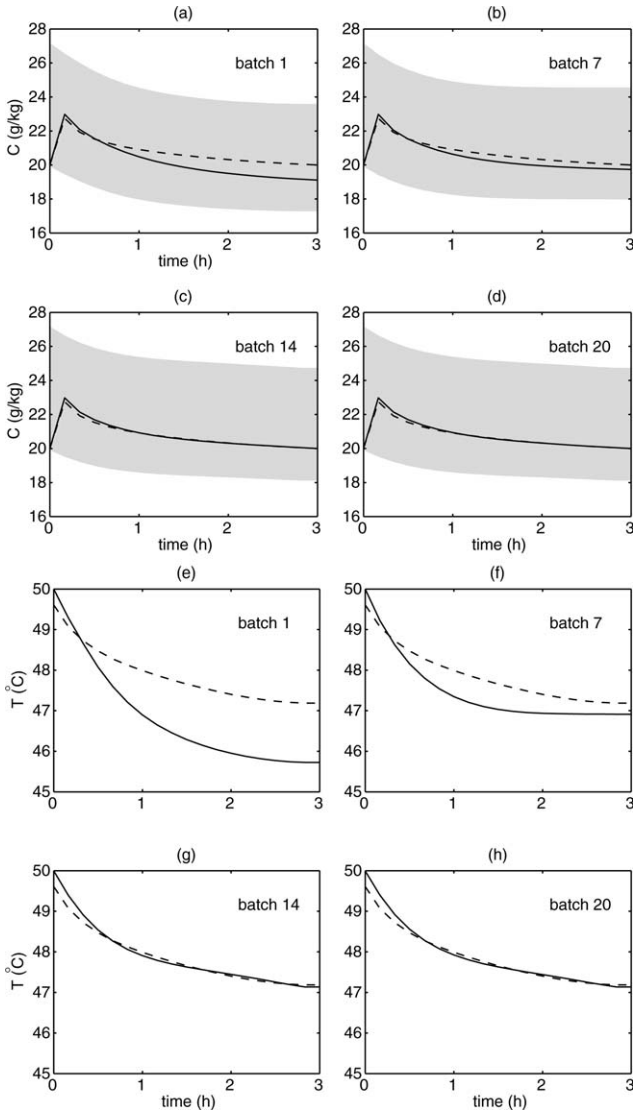

Figure 8. The results of applying the B2B control strategy for Case 1 and objective J_2 for batches 1, 7, 14, and 20.

(a)–(d) concentration trajectories with the shading showing the feasible region for the concentration; (e)–(h) the corresponding temperature trajectories. Solid line: B2B control, dashed line: optimal control.

(4) Obtain the step response coefficient matrices $\mathbf{G}_{pl}$ and $\mathbf{G}_{hl}$ by introducing a step change in $\boldsymbol{\delta u}$. Generally, the product quality measurement is only available at the end of the batch. Consequently, the PLS correction can only be calculated at the end of batch (i.e., for sampling instance N). To obtain $\mathbf{G}_{pl}$, the PLS correction for sampling instance N is added to the prediction of product quality at sampling instance k to $N - 1$.

(5) Obtain $\Pi^* = [\Delta\mathbf{U}_l^*, \epsilon^*]^T$ from the solution to the minimization (31) and (32), then update the elements of $\mathbf{U}_b$ by

$$u_{b,k+j}^{\text{new}} = u_{b,k+j}^{\text{old}} + \sum_{i=0}^{j} \Delta u_{l,k+i},$$

where $u_{b,k+j}^{\text{old}}$ and $u_{b,k+j}^{\text{new}}$ are the elements of $\mathbf{U}_b$ before and after updating, respectively, and $j = 0,\ldots,N - 1 + k$.

(6) If $err = \left\| \begin{bmatrix} \mathbf{G}_{pl} \\ \mathbf{G}_{hl} \end{bmatrix} \Delta\mathbf{U}_l^* \right\|$ is greater than a specified tolerance (1×10^{-4} was used in this study), $iter = iter + 1$, and repeat from Step 2. Otherwise set $\mathbf{U}_{\text{optimal}} = \mathbf{U}_b$ and implement the first element of $\mathbf{U}_{\text{optimal}}$ to the process.

(7) If the end of the current batch is reached, repeat from Step 1 and go to the next batch.

Simulation Results and Discussion

In the polymorphic transformation, both α- and β-form crystals were seeded according to a Gaussian distribution with parameter values given in Table 2. The initial solute concentration C_0 and maximum final solute concentration

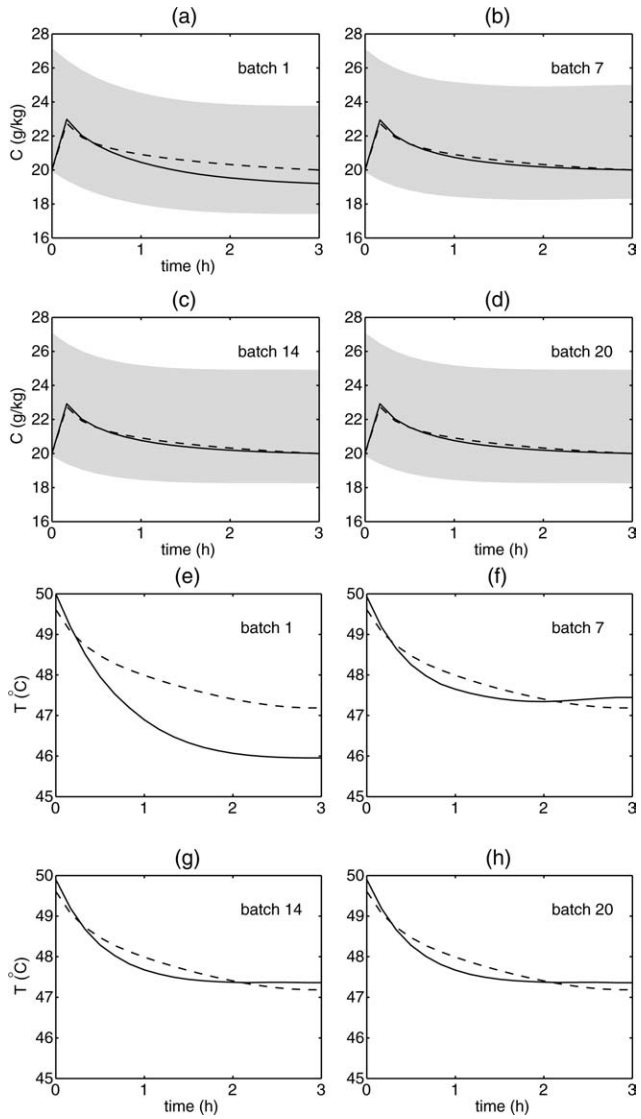

Figure 9. The results of applying the B2B-NMPC control strategy for Case 1 and objective J_2 for batches 1, 7, 14, and 20.

(a)–(d) concentration trajectories with the shading showing the feasible region for the concentration; (e)–(h) the corresponding temperature trajectories. Solid line: B2B-NMPC control, dashed line: optimal control.

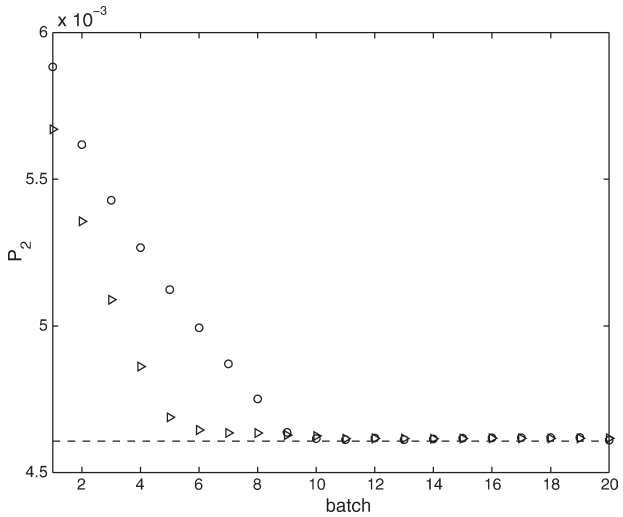

Figure 10. Comparison of the product quality P_2 obtained by the B2B (○) and B2B-NMPC (▷) control strategies for Case 1 and objective J_2.

$C_{\max}(t_f)$ are 20 g/kg. The batch time t_f was 3 hours and the sampling interval was 10 minutes.

Description of specific control implementations

The optimization of two different product qualities P_1 and P_2 was considered, which are associated with objectives J_1 and J_2, respectively. The process is assumed to be subject to two cases of parameter perturbations given in Table 3. The tuning parameters for the B2B and B2B-NMPC control strategies for both objectives are given in Tables 4 and 5, respectively. For all cases and objectives, the initial database (i.e., for the first batch) used for the PLS model comprised of historical operating data from ten batches. These batches included temperature trajectories around the nominal trajectory (see Supporting Information Figures S1–S4) obtained by optimizing the nominal first-principles model, the corresponding deviation between the measured concentration and the predicted concentration by the first-principles model, and the deviation values in final product quality. For the subsequent batches, the moving window approach was adopted to update the database, where up to 15 of the latest batches were kept in the database. For all cases and objectives, the temperature-time trajectory was parameterized as a first-order spline with 18 time intervals. The optimal trajectories shown as dashed lines in Figures 2–7 were obtained by optimizing the first-principles model with the set of perturbed parameters treated as known.

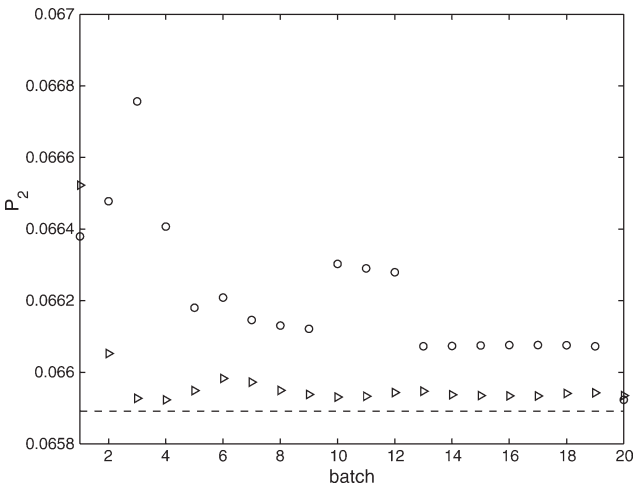

Figure 11. Comparison of the product quality P_2 obtained by the B2B (○) and B2B-NMPC (▷) control strategies for Case 2 and objective J_2.

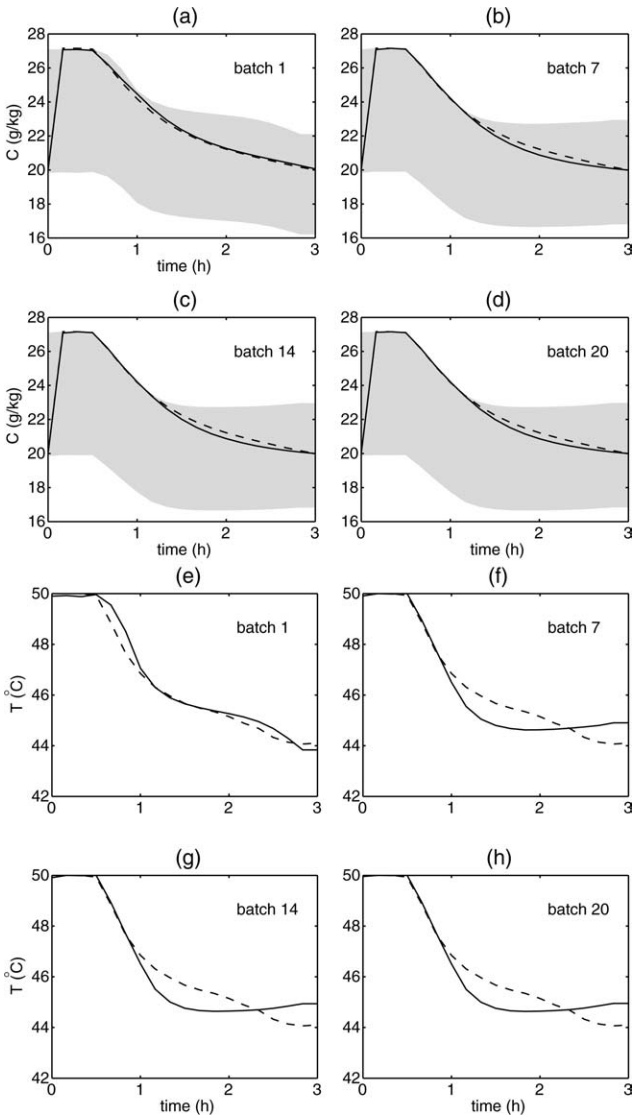

Figure 12. The results of applying the B2B control strategy for Case 2 and objective J_2 for batches 1, 7, 14, and 20.

(a)–(d) concentration trajectories with the shading showing the feasible region for the concentration; (e)–(h) the corresponding temperature trajectories. Solid line: B2B control, dashed line: optimal control.

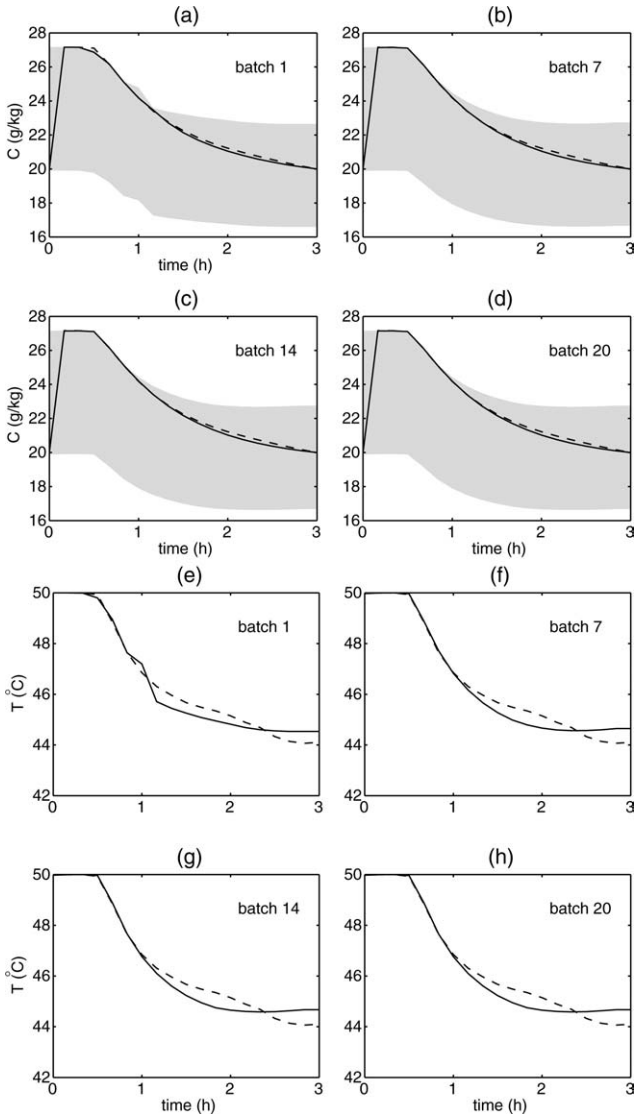

Figure 13. The results of applying the B2B-NMPC control strategy for Case 2 and objective J_2 for batches 1, 7, 14, and 20.

(a)–(d) concentration trajectories with the shading showing the feasible region for the concentration; (e)–(h) the corresponding temperature trajectories. Solid line: B2B-NMPC control, dashed line: optimal control.

Comparison results and discussion

For the first product quality objective P_1 to maximize the yield of β-form crystals, the optimal concentration trajectories for both cases are very close to the solubility curve of α-form crystals, which is one of the constraints. This is due to the slow growth rate of β-form crystals relative to the dissolution rate of α-form crystals. As a result, the optimal solution is to maximize the supersaturation with respect to the solubility of the β-form crystals while operating between the two solubility curves. Consequently, the nature of the optimal solution requires a control strategy that handles constraints well. For Case 1, the respective concentration and temperature trajectories for the B2B and B2B-NMPC control strategies in batches 1, 7, 14, and 20 are given by Figures 2 and 3. Both control strategies converge to optimality gradually and result in temperature and concentration trajectories very close to optimal at batch 20. Figure 4 compares the product quality P_1 obtained by both control strategies for batches 1 to 20. The product quality P_1 obtained by the B2B-NMPC control strategy has both faster and smoother convergence than for the B2B control strategy, which has a slight oscillation observed in batches 13 to 18. In addition, the B2B-NMPC control strategy satisfied all of the constraints for every batch, whereas the B2B control strategy violated one of the constraints during batches 5 to 8 (see Figure 4). For Case 2, the concentration and temperature trajectories for both control strategies in batches 1, 7, 14, and 20 are shown in Figures 5 and 6, where the convergence of both control strategies to optimality is shown. The trend in product quality shows similar observations as in Case 1 (see Figure 7), with the B2B-NMPC control strategy resulting in a faster convergence and satisfying all constraints, whereas the B2B control strategy violated one of the constraints in batch 2.

The product quality objective P_2 is more sophisticated than P_1. For P_1, the objective is to maximize the yield of the β-form crystals, which occurs by operating at maximum supersaturation to maximize the nucleation and growth rates of the β-form crystals. In contrast, P_2 is equivalent to maximizing the yield of the β-form crystals while minimizing their nucleation, which results in a tradeoff that needs to be maintained between the nucleation and growth rates of β-form crystals. As a result, the trajectories that optimize J_2 for both cases do not lie on either of the solubility curves. For Case 1, Figures 8 and 9 show the concentration and temperature trajectories for the B2B and B2B-NMPC control strategies, respectively. Although there is some difference between the temperature trajectories obtained by both control strategies and the optimal temperature trajectory in batch 20, the corresponding product quality P_2 obtained by both control strategies are very close to optimal (within 0.2%, see Figure 10). This comparison also suggests that the product quality P_2 is less sensitive to some variations in the temperature around the optimal temperature trajectory. As for P_1, the B2B-NMPC control strategy converged at a faster rate than the B2B control strategy (see Figure 10).

Figure 11 shows that the product quality P_2 in batch 20 obtained by the two control strategies for Case 2 are very close to optimal (within 0.1%), despite the differences in the concentration and temperature trajectories produced by the two control strategies and the corresponding optimal trajectories (see Figures 12 and 13). In addition, the convergence of the product quality P_2 obtained by the B2B-NMPC control strategy is much faster and smoother than that obtained by the B2B control strategy.

Conclusions

An integrated NMPC and batch-to-batch (B2B-NMPC) control strategy based on a hybrid model was developed for batch polymorphic crystallization processes. The performance of the proposed control strategy for optimizing two control objectives was evaluated for two cases of plant-model mismatch. The first objective aimed to maximize the yield of β-form crystals, whereas the second objective was

to minimize the ratio of nucleated crystal mass to seed crystal mass of β-form crystals. In a simulation study, the B2B-NMPC control strategy produced better performance compared to the standard B2B control strategy for all cases and objectives considered. In addition to satisfying all of the constraints, the convergence of the product quality obtained by the B2B-NMPC control strategy was consistently faster and smoother than that obtained by the B2B control strategy.

Literature Cited

1. Blagden N, Davey R. Polymorphs take shape. *Chem Br*. 1999;35:44–47.
2. Brittain HG. The impact of polymorphism on drug development: a regulatory viewpoint. *Am Pharm Rev*. 2000;3:67–70.
3. Fujiwara M, Nagy ZK, Chew JW, Braatz RD. First-principles and direct design approaches for the control of pharmaceutical crystallization. *J Process Control*. 2005;15:493–504.
4. Ma DL, Braatz RD. Robust identification and control of batch processes. *Comput Chem Eng*. 2003;27:1175–1184.
5. Nagy ZK, Braatz RD. Worst-case and distributional robustness analysis of finite-time control trajectories for nonlinear distributed parameter systems. *IEEE Trans Control Syst Technol*. 2003;11:694–704.
6. Nagy ZK, Braatz RD. Open-loop and closed-loop robust optimal control of batch processes using distributional and worst-case analysis. *J Process Control*. 2004;14:411–422.
7. Fujiwara M, Chow PS, Ma DL, Braatz RD. Paracetamol crystallization using laser backscattering and ATR-FTIR spectroscopy: metastability, agglomeration and control. *Cryst Growth Des*. 2002;2:363–370.
8. Nagy ZK, Chew JW, Fujiwara M, Braatz RD. Comparative performance of concentration and temperature controlled batch crystallizations. *J Process Control*. 2008;18:399–407.
9. Zafiriou E, Adomaitis RA, Gattu G. An approach to run-to-run control for rapid thermal processing. *Proc Am Control Conf*. 1995; 2:1286–1288.
10. Clarke-Pringle TL, MacGregor JF. Optimization of molecular-weight distribution using batch-to-batch adjustments. *Ind Eng Chem Res*. 1998;37:3660–3669.
11. Lee JH, Lee KS, Kim WC. Model-based iterative learning control with a quadratic criterion for time-varying linear systems. *Automatica*. 2000;36(5):641–657.
12. Doyle III FJ, Harrison CA, Crowley TJ. Hybrid model-based approach to batch-to-batch control of particle size distribution in emulsion polymerization. *Comput Chem Eng*. 2003;27:1153–1163.
13. Dokucu MT, Doyle III FJ. Batch-to-batch control of characteristic points on the PSD in experimental emulsion polymerization. *AIChE J*. 2008;54:3171–3187.
14. Xiong Z, Zhang J. A batch-to-batch iterative optimal control strategy based on recurrent neural network models. *J Process Control*. 2005;15:11–21.
15. Li C, Zhang J, Wang G. Batch-to-batch optimal control of batch processes based on recursively updated nonlinear partial least squares models. *Chem Eng Commun*. 2007;194:261–279.
16. Chin IS, Lee KS, Lee JH. A technique for integrated quality control, profile control, and constraint handling for batch processes. *Ind Eng Chem Res*. 2000;39:693–705.
17. Lee K, Lee JH, Yang DR, Mahoney AW. Integrated run-to-run and on-line model-based control ofparticle size distribution for a semi-batch precipitation reactor. *Comput Chem Eng*. 2002;26:1117–1131.
18. Lee KS, Chin IS, Lee HJ, Lee JH. Model predictive control technique combined with iterative learning for batch processes. *AIChE J*. 1999;45:2175–2187.
19. Chin I, Qin SJ, Lee KS, Cho M. A two-stage iterative learning control technique combined with real-time feedback for independent disturbance rejection. *Automatica*. 2004;40:1913–1922.
20. De Keyser RMC. *Model based predictive control for linear systems*. In: *UNESCO Encyclopaedia of Life Support Systems*. Oxford: EOLLS Publishers Co Ltd. 2003.
21. De Keyser RMC, Cauwenberghe ARV. *Extended prediction self-adaptive control*. In: *IFAC Symposium on Identification and System Parameter Estimate*. IFAC; 1985; 1255–1260.
22. Ionescu C, De Keyser RMC. EPSAC predictive control of blood glucose level in type I diabetic patients. Proceedings of the 44th Conference on Decision and Control, and the European Control Conference, IEEE, New York; 2005; 4845–4850.
23. Rueda A, Cristea S, Prada CD, De Keyser RMC. Non-linear predictive control for a distillation column. Proceedings of the 44th IEEE conference on Decision and Control, and the European Control Conference, IEEE, New York. 2005; 5156–5161.
24. Hermanto MW, Kee NC, Tan RBH, Chiu MS, Braatz RD. Robust Bayesian estimation of kinetics for the polymorphic transformation of L-glutamic acid crystals. *AIChE J*. 2008;54:3248–3259.
25. Mersmann A. *Crystallization technology handbook*. Florida, 2nd ed. USA: CRC Press, 2001.
26. Hermanto MW, Braatz RD, Chiu MS. High-order simulation of polymorphic crystallization using weighted essentially nonoscillatory methods. *AIChE J*. 2009;55:122–131.
27. Rawlings JB, Miller SM, Witkowski WR. Model identification and control of solution crystallization processes: a review. *Ind Eng Chem Res*. 1993;32:1275–1296.
28. Togkalidou T, Tung HH, Sun Y, Andrews A, Braatz RD. Solution concentration prediction for pharmaceutical crystallization processes using robust chemometrics and ATR FTIR spectroscopy. *Org Process Res Dev*. 2002;6:317–322.
29. Wold S, Kettaneh-Wold N, Skagerberg B. Nonlinear PLS modeling. *Chemom Intell Lab Syst*. 1989;7:53–65.
30. Lampinen J. *A constraint handling approach for the differential evolution algorithm*. Proceedings of the 2002 Congress on Evolutionary Computation, vol. 2. Washington, DC: IEEE; 2002; 1468–1473.
31. Storn R, Price K. Differential evolution-a simple and efficient heuristic for global optimization over continuous spaces. *J Global Optim*. 1997;11:341–359.
32. Scokaert POM, Rawlings JB. Feasibility issues in linear model predictive control. *AIChE J*. 1999;45:1649–1659.

Manuscript received Jun. 4, 2009, and revision received May 17, 2010.